ELSEVIER

Deep-Sea Research II 51 (2004) 139–146

DEEP-SEA RESEARCH
PART II

www.elsevier.com/locate/dsr2

Ocean-color variability in the Gulf of California: scales from days to ENSO

Mati Kahru[a,*], S.G. Marinone[b], S.E. Lluch-Cota[c], Alejandro Parés-Sierra[b], B. Greg Mitchell[a]

[a] *Scripps Institution of Oceanography, University of California San Diego, La Jolla, CA 92093-0218, USA*
[b] *Departamento de Oceanografia Fisica, CICESE, Ensenada, CP 22860, B.C., Mexico*
[c] *Centro de Investigaciones Biologicas del Noroeste, S.C. P.O. Box 128, La Paz, BCS, 23000, Mexico*

Received 8 August 2002; received in revised form 9 April 2003; accepted 9 April 2003

Abstract

Time series of surface chlorophyll *a* concentration (C_{sat}) and phytoplankton net primary production (NPP) in the Gulf of California were derived using satellite data from OCTS, SeaWiFS, MODIS, AVHRR and the VGPM primary productivity model. The 6-year (1997–2003) time series showed variability at a multitude of scales. The annual cycle was the dominant mode in C_{sat} variability in the entire gulf, except just south of the midriff islands where the semiannual cycle dominated. The semiannual cycle has C_{sat} maxima during the spring and fall transition periods when the general circulation is switching between cyclonic in the summer and anticyclonic in the winter and is less developed, therefore allowing a more efficient tidal mixing. The spring and fall maxima often consisted of multiple peaks of about 10 days. A significant peak at about 1 month was often present in the short-term C_{sat} variability, especially in areas near the midriff islands, suggesting the influence of tidal mixing. The interannual variability was dominated by the 1997–98 El Niño and the following La Niña. During the El Niño period NPP decreased by 30–40% in the southern part of the gulf (by approximately 1 Tg C month^{-1}), but the changes in the central and northern parts were less evident.
© 2004 Elsevier Ltd. All rights reserved.

1. Introduction

The Gulf of California is a subtropical, semi-enclosed sea with exceptionally high primary productivity and important commercial fisheries (Zeitzschel, 1969). Topographically the Gulf of California consists of a series of basins. The shallow northern part is separated from the deeper southern part by a sill and the midriff islands. High productivity in the gulf is the result of efficient nutrient transport into the euphotic zone (Valdez-Holguín and Lara-Lara, 1987). The main mechanisms of nutrient enrichment are tidal stirring and coastal upwelling. The region of the midriff islands of Angel de la Guarda and Tiburón, delimited to the south by a sill, is the most important area of mixing due to strong tidal stirring, breaking internal waves, and possibly internal hydraulic jumps (Roden and Groves, 1959; Paden et al., 1991; Luch-Cota, 2000). The Gulf of California has been an ideal site for satellite remote sensing due to the special

*Corresponding author. Tel.: +1-858-534-8947; fax: +1-858-534-2997.
E-mail address: mkahru@ucsd.edu (M. Kahru).

0967-0645/$ - see front matter © 2004 Elsevier Ltd. All rights reserved.
doi:10.1016/j.dsr2.2003.04.001

meteorological conditions, leading to frequent cloud-free conditions (e.g., Paden et al., 1991; Santamaría-del-Angel et al., 1994a, b).

The high spatial and temporal variability inherent in most oceanic fields severely limits our ability to detect changes using conventional shipboard measurements. Primary production measurements are known to have particularly high variability (Mantyla et al., 1995; Valdez-Holguín and Lara-Lara, 1987), which makes detecting trends and responses to environmental factors very difficult with shipboard measurements alone. Satellite remote sensing coupled with models is a powerful tool that can resolve spatial and temporal variability over large areas. Several models of phytoplankton net primary production (NPP, g C month^{-1}) have been developed and successfully implemented (e.g., Behrenfeld and Falkowski, 1997; Behrenfeld et al., 2001). We applied the Behrenfeld–Falkowski vertically generalized production model (VGPM) to satellite-derived fields of surface chlorophyll *a* concentration (C_{sat} mg m^{-3}), incident photosynthetically active radiation (PAR, Einstein m^{-2} Day^{-1}), and sea-surface temperature (SST, °C) to derive a 6-year time series of C_{sat} and NPP to study their temporal and spatial variability in the Gulf of California.

2. Data and methods

Time series were constructed for 12 sub-areas that were expected to have coherent dynamics of the surface chlorophyll *a* concentration. The sub-areas were initially defined by cluster analysis of the mean annual cycle of C_{sat} based on the Coastal Zone Color Scanner climatology, minimizing differences between pixels of each group and maximizing differences between groups (Fig. 1). The clusters define regions with similar annual cycle of C_{sat} and are assumed to be influenced by the same processes.

As an estimate of the surface chlorophyll *a* concentration we used the standard mapped images of C_{sat} from OCTS (NASDA, 1997; data reprocessed by NASA) and SeaWiFS (processing version 4) as produced and distributed by the Goddard Distributed Active Archive Center. Both

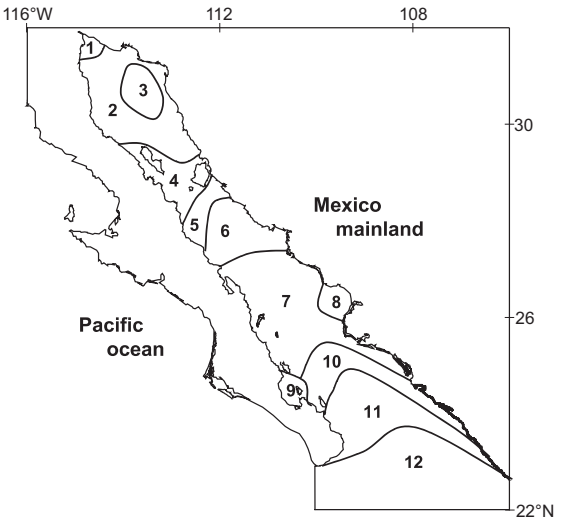

Fig. 1. Sub-areas 1–12 in the Gulf of California.

the OCTS (Nov. 1996–June 1997) and SeaWiFS (Sept. 1997–Oct. 2003) estimates of C_{sat} were derived using standard algorithms (O'Reilly et al., 1998, 2000). Time series of C_{sat} and NPP in each area were based on the median of all valid pixels in the area.

The VGPM model was run on monthly composited fields of C_{sat}, PAR and SST with a spatial resolution of approximately 9 km. PAR fields were calculated by NASA from SeaWiFS data with the Frouin algorithm (http://orca.gsfc.nasa.gov/seawifs/par/doc/seawifs_par_wfigs.pdf). For the OCTS time period PAR fields were not available due to that sensor's saturation over clouds, and we used the mean monthly PAR fields from SeaWiFS instead. A simple sensitivity experiment showed that the interannual variability in monthly PAR was small and had only a minor effect on the calculated NPP. SST was derived from the AVHRR Pathfinder daytime products (Kilpatrick et al., 2001), except for the period after Aug. 2002 when we used MODIS daytime 11-μm products.

Monthly NPP for each sub-area was calculated by multiplying each valid pixel's value by the pixel area and integrating over all valid pixels in the sub-area. The integrated NPP values for each sub-area were adjusted for the missing values due to clouds by multiplying the total NPP for valid pixels to the

ratio of total area to the area of valid pixels. Integral NPP and their differences were expressed in Tg C month^{-1} (Tg = 10^{12} g). Anomalies (relative to the mean annual cycle) were calculated by subtracting the mean annual cycle for each sub-area from the actual monthly values. The mean annual cycle was calculated by fitting a 6th degree polynomial through all the data points expressed as a function of the day of the year for each of the 12 areas. For the calculation of annual total NPP we used the sum of 12 monthly NPP values from July to June of the next year to correspond better with the El Niño-La Niña cycle.

As an index of the El Niño-La Niña cycle we used the Northern Oscillation Index (NOI) calculated from the difference between anomaly sea-level pressures at 35°N, 135°W and 10°S, 130°E (Schwing et al., 2002). The El Niño periods are defined as minima in NOI. We smoothed the NOI time series with a 3-month running average. In general we refer to the second half of 1997 and first half of 1998 as the El Niño period (shown with black bars on Fig. 5) and the period from late 1998 through the first half of 1999 as the La Niña period. Another El Niño period started to develop in Oct. 2002.

For detecting periodicities in time series, we used the Lomb normalized periodograms (Lomb, 1976; Press et al., 1992).

3. Results

Medians of the monthly C_{sat} for each of the sub-areas are shown in Fig. 2. The annual cycle was the dominant period of variability in all of the sub-areas, except sub-areas 4 and 5 (Fig. 3). In the region of the midriff islands (sub-areas 4 and 5) a mode with a period of 6 months contained more variance than the annual cycle whereas in sub-area 5 this mode dominated and the annual cycle was totally masked. The annual minimum in C_{sat} in all sub-areas occurred in mid-summer (typically in July) while in sub-areas 4 and 5 a secondary minimum occurred in mid-winter (January). The maxima in the region of the midriff islands occurred during the spring and fall transition periods and typically consisted of a series of pulses of increased concentration lasting about 10 days (Fig. 4). During the 3–4 month transition period there were typically 3–4 such pulses. At times the maxima in C_{sat} appear to be separated by about 14 days that corresponds to the spring/neap tide cycle. Calculated Lomb spectra (not shown) based on daily C_{sat} confirm the existence of a dominant period of about 1 month, which is also one of the tidal periods (the Mm constituent). However, similar pulses of high C_{sat} were also observed in sub-area 8 where other factors, such as coastal upwelling events and the passage of baroclinic eddies, are expected to have a strong influence.

The inter-annual component in C_{sat} variability was present in all sub-areas but more evident in the southern half of the gulf. The length of the summer minimum in C_{sat} was considerably longer during the El Niño year of 1998 (Fig. 4). A reduction of both C_{sat} and NPP was associated with the 1997–1998 El Niño event, especially in the southern sub-areas (Fig. 5). To facilitate generalizations we added the integrated monthly NPP values for sub-areas with similar dynamics. Areas 1–3 correspond to the shallow northern gulf, areas 4–5 to the tidally energetic islands and sills region, areas 6–9 to the central deeper gulf, and areas 10–12 in the mouth area with the strongest influence of the Pacific (see for example, Soto-Mardones et al., 1999).

The areas of the combined sub-regions are shown in Table 1. In sub-areas 10–12 the monthly NPP was consistently lower than the long-term monthly mean by 30–40% during the second half of 1997 and throughout most of 1998 (Fig. 6), corresponding to a decrease of approximately 1 Tg C month^{-1} relative to the mean annual cycle. In the northern sub-areas (1–3 and 4–5) the effect of the El Niño on NPP was less evident.

The total NPP integrated over the entire gulf was highest during the spring of 2001 and peaked in April 2001 at 23 Tg C month^{-1}. The lowest total NPP in August 1998 (3.7 Tg C month^{-1}) occurred during the summer minimum following the El Niño event. The maximum of the annual total NPP was observed during 2000–2001 while the minimum occurred during the El Niño year of 1997–1998 (Table 2).

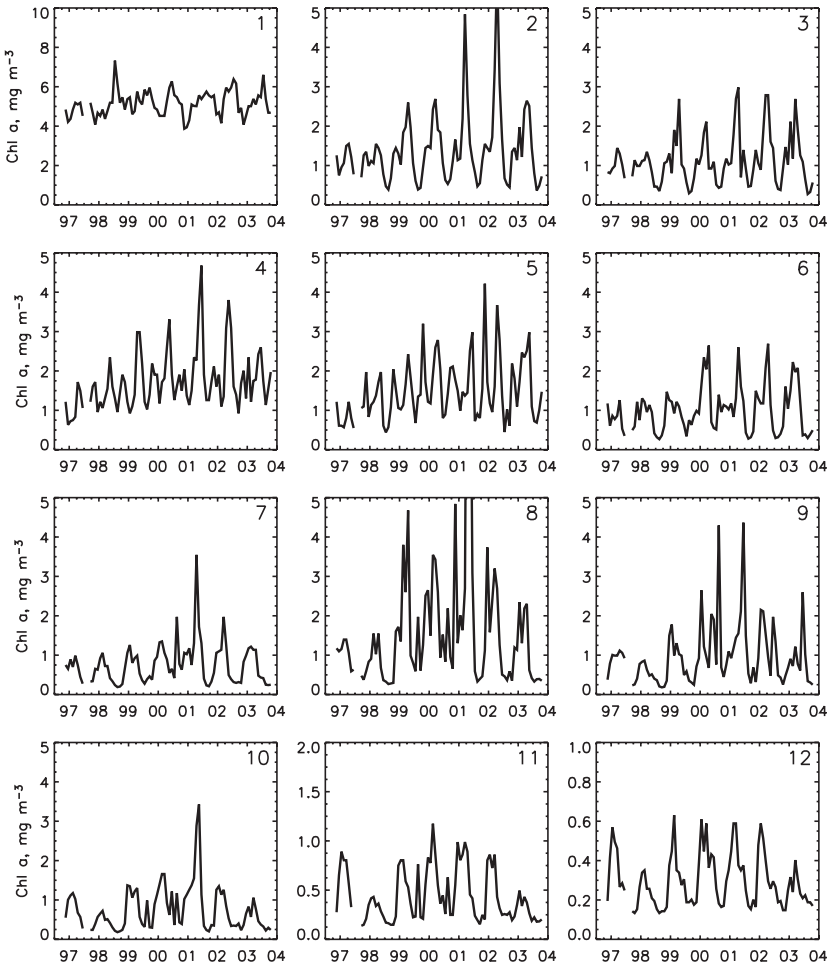

Fig. 2. Monthly time series of C_{sat} in sub-areas 1–12 showing the median for each sub-area.

4. Discussion and conclusions

In this paper we have quantified different modes of variability in C_{sat} and NPP in the Gulf of California based primarily on remotely sensed data from SeaWiFS. Even though the calculated NPP fields depend on SST, PAR and daylength, C_{sat} dominated the variability in NPP. The annual cycle is the dominant period of variability everywhere except just south of the midriff islands where the semiannual cycle dominated. The spring and fall maxima in C_{sat} appear as a series of approximately 10-day pulses of increased concentration during the 3–4 month transition periods when the general circulation is known to switch between cyclonic during summer and anticyclonic during winter (Bray, 1988; Beier, 1997). The exact mechanism of these high C_{sat} pulses and the resulting approximately 1-month peak in the variance spectra is not clear, but it may be caused by the fortnightly variation of the tidal energy with stronger spring tides once a month resulting in enhanced mixing. The fact that the semiannual cycle dominates in the midriff islands region and not elsewhere supports the hypothesis that the semiannual maxima are produced by the effect of tidal mixing. In the spring and fall, when the vertical thermohaline stratification is relatively weak, tidal mixing with its fortnightly and monthly modulation is effective in pumping

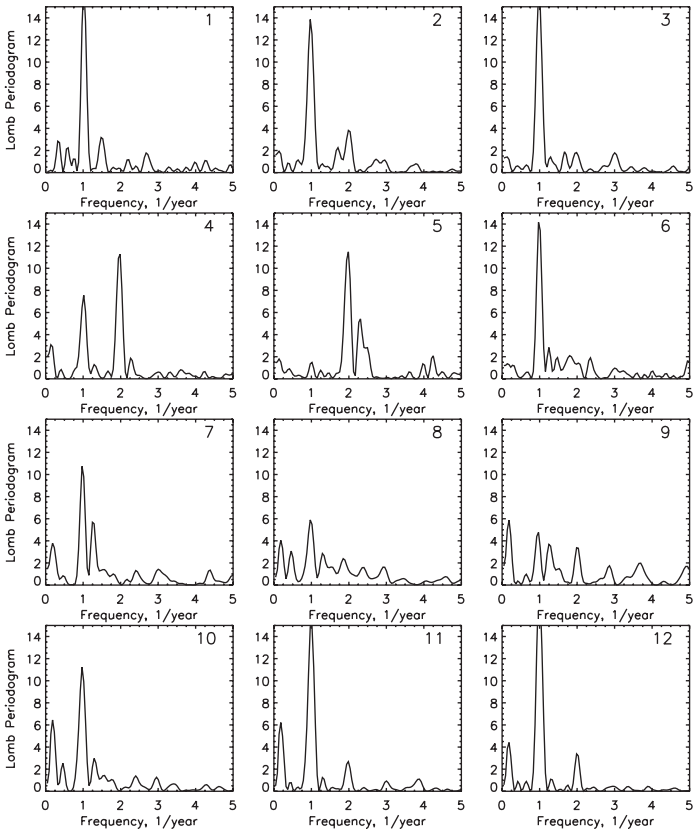

Fig. 3. Lomb normalized periodograms of C_{sat} in sub-areas 1–12.

nutrients into the surface layer and triggering the phytoplankton blooms. During the summer vertical mixing is suppressed by the strong stratification and the supply of nutrients is limited. Furthermore, a simulation with a numerical circulation model (Marinone, 2003) shows strong southward (northward) currents during mid-summer (mid-winter), which advect waters of relatively low C_{sat} to the islands region from the neighboring areas, i.e. from sub-area 2 in the summer and sub-area 6 in the winter (see Fig. 2). The semiannual cycle, being stronger in the islands region than elsewhere, also was observed by Soto-Mardones et al. (1999) in SST. Paden et al. (1991) also found bimodal variability in SST patterns in the islands region and explained it by the two maxima in the annual tidal range. However, the period between the 2 annual peaks (April–May and July–August) observed by Paden et al. (1991) was only 3 months whereas the semiannual cycle observed in this paper was symmetric in time with 6 months between the maxima.

Pegau et al. (2002) observed a series of quasi-stationary eddies between the midriff islands and the mouth of the gulf that had an alternative sense of rotation and appeared to dominate the surface circulation and C_{sat} distribution. These eddies must obviously influence the temporal variability in C_{sat} and NPP examined in this paper, but the relationship between the temporal patterns and the quasi-stationary eddies needs further studies.

Previous studies in the California Current (Fiedler, 1984; Strub et al., 1990; Thomas et al., 1994; Kahru and Mitchell, 2000, 2002) have shown that El Niño events reduce the upwelling of nutrient-rich waters and the extent of high-chlorophyll surface waters. However, offshore waters off Baja California have been shown to

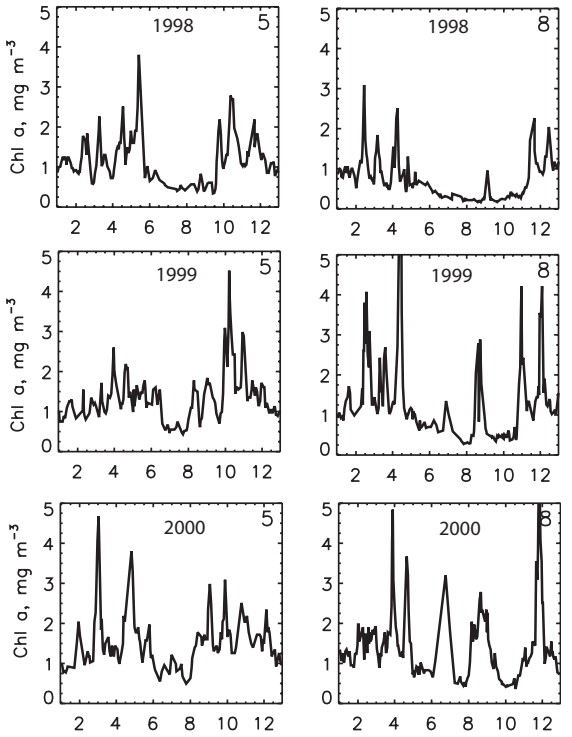

Fig. 4. Annual time series of C_{sat} in sub-areas 5 and 8 for 1998, 1999 and 2000 based on daily images.

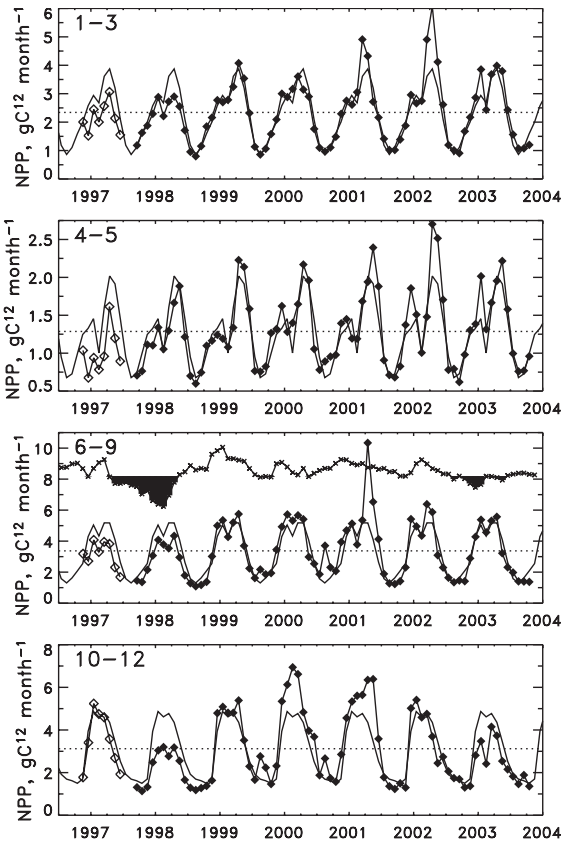

Fig. 5. Time series of NPP in the combined sub-areas 1–3, 4–5, 6–9, 10–12 calculated with C_{sat} from OCTS (◇) and SeaWiFS (◆) and compared with the mean annual cycle (solid line). The Northern Oscillation Index (×, relative scale, in the third panel) values below −1 are shown with black bars and correspond to the El Niño period.

Table 1
Areas of the combined sub-areas used in the NPP calculations

Combined sub-areas	Area (km^2)
1–3	39,237
4–5	19,886
6–9	72,605
10–12	110,263

have a contrary pattern of increased surface chlorophyll and primary production during both of the last major El Niño events of 1982–1984 and 1997–1998 (Kahru and Mitchell, 2000, 2002). The interannual variability in the Gulf of California (Table 2) is higher than in the broad region of the California Current. The coefficient of variation in annual NPP is nearly 17% in the Gulf of California versus only 4.4% in the California Current. We observed a 30–40% decrease in NPP in the southern half of the Gulf of California during and immediately following the 1997–98 El Niño. The response in the central and northern gulf was also negative during and immediately after the El Niño but the correlation with NOI was less obvious. Significant negative anomaly in the central and northern gulf was also observed before the El Niño (as detected by NOI) but some of that may have been caused by the differences between OCTS and SeaWiFS algorithms. The drastic decrease in NPP (especially in the southern half of the Gulf of California) associated with the El Niño must have significant consequences for the higher trophic levels. These results are in accordance with the conclusions of Santamaría-del-Angel et al. (1994b) who observed a similar pattern of decreased surface pigments in the southern part

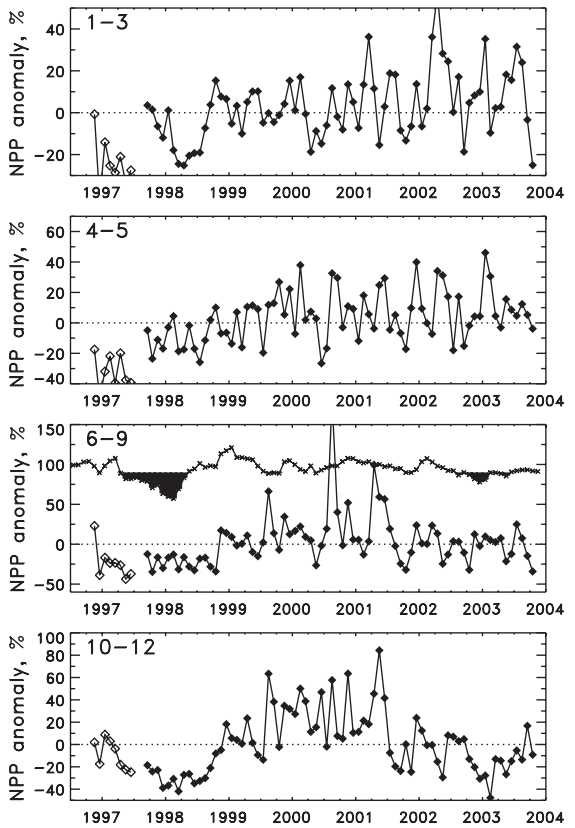

Fig. 6. Anomalies of NPP (%) in the combined sub-areas 1–3, 4–5, 6–9, 10–12 calculated with C_{sat} from OCTS (◇) and SeaWiFS (♦) relative to the mean annual cycle. The Northern Oscillation Index (×, relative scale, in the third panel) values below −1 are shown with black bars and correspond to the El Niño period.

of the gulf during the 1982–1984 El Niño using the Coastal Zone Color Scanner data. The exact mechanisms causing reduced C_{sat} and NPP in the Gulf of California during El Niño events are not clear but both the intrusion of tropical surface waters with lower chlorophyll content (Castro, 2001) and the reduction of vertical mixing due to increased thermal stratification are probably relevant.

Acknowledgements

Financial support to MK and BGM was provided by NASA (NAG5-6559). We thank the SeaWiFS Project and the distributed active archive center (DAAC) for the SeaWiFS, OCTS and MODIS data, and the Jet Propulsion Laboratory DAAC for SST data.

Table 2
Estimated total annual NPP for the Gulf of California (monthly totals were added from July to June of the next year, missing months were substituted with a corresponding mean), mean NPP for the whole Gulf of California as compared to the California Current region

Year	Annual NPP (10^{12} g C yr^{-1})	Mean NPP (g C m^{-2} yr^{-1})	Mean NPP (g C m^{-2} yr^{-1}) for the California current
1996–1997	100	420	180
1997–1998	96	403	192
1998–1999	120	505	195
1999–2000	135	565	198
2000–2001	148	622	199
2001–2002	126	530	205
2002–2003	119	499	200

The California Current values are adapted from Kahru and Mitchell (2002) and are for the 0–1000 km band along the coast between Cape Mendocino and Cabo San Lucas.

References

Behrenfeld, M.J., Falkowski, P.G., 1997. Photosynthetic rates derived from satellite-based chlorophyll concentration. Limnology and Oceanography 42, 1–20.

Behrenfeld, M.J., Randerson, J.T., McClain, C.R., Feldman, G.C., Los, S.O., Tucker, C.J., Falkowski, P.G., Field, C.B., Frouin, R., Esaias, W.E., Kolber, D.D., Pollack, N.H., 2001. Biospheric primary production during an ENSO transition. Science 291, 2594–2597.

Beier, E., 1997. Numerical investigation of the annual variability in the Gulf of California. Journal of Physical Oceanography 27, 615–632.

Bray, N.A., 1988. Thermohaline circulation in the Gulf of California. Journal of Geophysical Research 93, 4993–5020.

Castro, R., 2001. Variabilidad termohalina e intercambios de calor, sal y agua en la entrada al Golfo de California. Ph.D. Thesis, UABC, Ensenada, México.

Fiedler, P.C., 1984. Satellite observations of the 1982–1983 El Niño along the U.S. Pacific coast. Science 224, 1251–1254.

Kahru, M., Mitchell, B.G., 2000. Influence of the 1997–98 El Niño on the surface chlorophyll in the California current. Geophysical Research Letters 27, 2937–2940.

Kahru, M., Mitchell, B.G., 2002. Influence of the El Niño–La Niña cycle on satellite-derived primary production in the California current. Geophysical Research Letters 29(9), doi:10.1029/2002GL014963.

Kilpatrick, K.A., Podesta, G.P., Evans, R.H., 2001. Overview of the NOAA/NASA AVHRR Pathfinder algorithm for sea surface temperature and associated matchup database. Journal of Geophysical Research 106 (C5), 9179–9197.

Lomb, N.R., 1976. Least-squares frequency analysis of unequally spaced data. Astrophysics and Space Science 39, 447–462.

Luch-Cota, S.-E., 2000. Coastal upwelling in the eastern Gulf of California. Oceanologica Acta 23 (6), 731–740.

Mantyla, A.W., Venrick, E.L., Hayward, T.L., 1995. Primary production and chlorophyll relationships, derived from ten years of CalCOFI measurements. California Cooperative Oceanic and Fisheries Investigations Reports 36, 159–166.

Marinone, S.G., 2003. A three-dimensional model of the mean and seasonal circulation of the gulf of california. Journal of Geophysical Research 108 (C10), 3325 [doi:10.1029/2002JC001720].

NASDA, 1997. Advanced Earth Observing Satellite (ADEOS). OCTS Data Processing Algorithm Description, Ver. 2.0.1, NASDA Earth Observation Center, Tokyo, Japan.

O'Reilly, J.E., Maritorena, S., Mitchell, B.G., Siegel, D.A., Carder, K.L., Garver, S.A., Kahru, M., McClain, C.R., 1998. Ocean color chlorophyll algorithms for SeaWiFS. Journal of Geophysical Research 103, 24937–24953.

O'Reilly, J.E., et al., 2000. Ocean color chlorophyll *a* algorithms for SeaWiFS, OC2, and OC4: Version 4. NASA Technical Memorandum, 2000-206892, 11, 9–23.

Paden, C.A., Abbott, M.R., Winant, C.D., 1991. Tidal and atmospheric forcing of the upper ocean in the Gulf of California 1. Sea surface temperature variability. Journal of Geophysical Research 96 (C10), 18337–18359.

Pegau, W.S., Boss, E., Martinez, A., 2002. Ocean color observations of eddies during the summer in the Gulf of California. Geophysical Research Letters 29, 10.1029/2001GL014076.

Press, W.H., Tuekolsky, S.A., Wettering, W.T., Flannery, B.P., 1992. Numerical Recipes in C: The Art of Scientific Computing, 2nd Edition, Cambridge University Press, New York. 994pp.

Roden, G.I., Groves, G.W., 1959. Recent oceanographic observations in the Gulf of California. Journal of Marine Research 18, 10–35.

Santamaría-del-Angel, E., Alvarez-Borrego, S., Müller-Karger, F.E., 1994a. Gulf of California bio-geographic regions based on coastal zone color scanner imagery. Journal of Geophysical Research 99 (C4), 7411–7421.

Santamaría-del-Angel, E., Alvarez-Borrego, S., Müller-Karger, F.E., 1994b. The 1982–1984 El Niño in the Gulf of California as seen in the coastal zone color scanner imagery. Journal of Geophysical Research 99 (C4), 7423–7431.

Schwing, F.B., Murphree, T., Green, P.M., 2002. The Northern Oscillation Index (NOI): a new climate index for the northeast Pacific. Progress in Oceanography 53, 115–139.

Soto-Mardones, L., Marinone, S.G., Parés-Sierra, A., 1999. Time and spatial variability of sea surface temperature in the Gulf of California. Ciencias Marinas 25, 1–30.

Strub, P.T, James, C., Thomas, A.C., Abbott, M.R., 1990. Seasonal and nonseasonal variability of satellite-derived surface pigment concentration in the California Current. Journal of Geophysical Research 95, 11501–11530.

Thomas, A.C., Huang, F., Strub, P.T., James, C., 1994. Comparison of the seasonal and interannual variability of phytoplankton pigment concentrations in the Peru and California Current systems. Journal of Geophysical Research 99, 7355–7370.

Valdez-Holguín, J.E., Lara-Lara, R., 1987. Primary productivity in the Gulf of California: effects of El 1982–1983 event. Ciencias Marinas 13, 34–50.

Zeitzschel, B., 1969. Primary productivity in the Gulf of California. Marine Biology 3, 201–207.